AFRL-RX-WP-TP-2008-4035

MODELING PITTING AND CORROSION PHENOMENA BY EDDY-CURRENT VOLUME-INTEGRAL EQUATIONS (POSTPRINT)

Harold A. Sabbagh, Elias H. Sabbagh, R. Kim Murphy, John C. Aldrin, Eric Lindgren, and Jeremy S. Knopp

Nondestructive Evaluation Branch
Metals, Ceramics & Nondestructive Evaluation Division

DECEMBER 2006

AIR FORCE RESEARCH LABORATORY
MATERIALS AND MANUFACTURING DIRECTORATE
WRIGHT-PATTERSON AIR FORCE BASE, OH 45433-7750
AIR FORCE MATERIEL COMMAND
UNITED STATES AIR FORCE

REPORT DOCUMENTATION PAGE

Form Approved
OMB No. 0704-0188

1. REPORT DATE *(DD-MM-YY)*	2. REPORT TYPE	3. DATES COVERED *(From - To)*
December 2006	Conference Proceedings Postprint	

4. TITLE AND SUBTITLE
MODELING PITTING AND CORROSION PHENOMENA BY EDDY-CURRENT VOLUME-INTEGRAL EQUATIONS (POSTPRINT)

5a. CONTRACT NUMBER
In-house

5b. GRANT NUMBER

5c. PROGRAM ELEMENT NUMBER
62102F

6. AUTHOR(S)
Harold A. Sabbagh, Elias H. Sabbagh, and R. Kim Murphy (Victor Technologies, LLC)
John C. Aldrin (Computational Tools)
Eric Lindgren and Jeremy S. Knopp (AFRL/RXLP)

5d. PROJECT NUMBER
4349

5e. TASK NUMBER
RG

5f. WORK UNIT NUMBER
M04R1000

7. PERFORMING ORGANIZATION NAME(S) AND ADDRESS(ES)
Victor Technologies, LLC
P.O. Box 7706
Bloomington, IN 47407-7706

Computational Tools
Gurnee, IL 60031

Nondestructive Evaluation Branch (AFRL/RXLP)
Metals, Ceramics & Nondestructive Evaluation Division
Materials and Manufacturing Directorate
Wright-Patterson Air Force Base, OH 45433-7750
Air Force Materiel Command
United States Air Force

8. PERFORMING ORGANIZATION REPORT NUMBER
AFRL-RX-WP-TP-2008-4035

9. SPONSORING/MONITORING AGENCY NAME(S) AND ADDRESS(ES)
Air Force Research Laboratory
Materials and Manufacturing Directorate
Wright-Patterson Air Force Base, OH 45433-7750
Air Force Materiel Command
United States Air Force

10. SPONSORING/MONITORING AGENCY ACRONYM(S)
AFRL/RXLP

11. SPONSORING/MONITORING AGENCY REPORT NUMBER(S)
AFRL-RX-WP-TP-2008-4035

12. DISTRIBUTION/AVAILABILITY STATEMENT
Approved for public release; distribution unlimited.

13. SUPPLEMENTARY NOTES
Conference paper published in the Proceedings of the 23rd Annual Review of Progress in Applied Computational Electromagnetics. Paper contains color.

 PAO Case Number: AFRL/WS 07-0070, 23 Jan 2007.

14. ABSTRACT
A wide variety of problem in computational electromagnetics has been successfully solved using a volume-integral approach along with conjugate-gradient methods. In the arena of quantitative nondestructive evaluation (NDE) of nuc1ear-power and aerospace structures, the problem of modeling pitting and corrosion phenomena is particularly challenging. Based on real corrosion pits in heat-exchanger tubes in nuclear power plants, and manufactured pits in aircraft structures, we develop general models that are suitable for the analysis using VIC-3D©, a proprietary volume-integral code. Based on these models, we develop the notion of model-based inversion, and apply it to the NDE of corrosion and pitting phenomena.

15. SUBJECT TERMS
Volume-integral equations, electromagnetic nondestructive evaluation, corrosion and pitting phenomena, model-based inversion

16. SECURITY CLASSIFICATION OF:			17. LIMITATION OF ABSTRACT:	18. NUMBER OF PAGES	19a. NAME OF RESPONSIBLE PERSON (Monitor)
a. REPORT	b. ABSTRACT	c. THIS PAGE			Kumar Jata
Unclassified	Unclassified	Unclassified	SAR	14	19b. TELEPHONE NUMBER *(Include Area Code)* N/A

Standard Form 298 (Rev. 8-98)
Prescribed by ANSI Std. Z39-18

MODELING PITTING AND CORROSION PHENOMENA BY EDDY-CURRENT VOLUME-INTEGRAL EQUATIONS

Harold A. Sabbagh, Elias H. Sabbagh and R. Kim Murphy
has@sabbagh.com, ehs@sabbagh.com, kimmurphy1@aristotle.net
Victor Technologies, LLC
PO Box 7706
Bloomington, IN 47407-7706 USA

John C. Aldrin
aldrin@computationaltools.com
Computational Tools
Gurnee, IL 60031 USA

Eric Lindgren
Eric.Lindgren@wpafb.af.mil
Air Force Research Laboratory (AFRL/MLLP)
Wright-Patterson AFB, OH 45433-7817 USA

Jeremy S. Knopp
Jeremy.Knopp@wpafb.af.mil
Air Force Research Laboratory (AFRL/MLLP)
Wright-Patterson AFB, OH 45433-7817 USA

Abstract: A wide variety of problems in computational electromagnetics has been successfully solved using a volume-integral approach along with conjugate-gradient methods. In the arena of quantitative nondestructive evaluation (NDE) of nuclear-power and aerospace structures, the problem of modeling pitting and corrosion phenomena is particularly challenging. Based on real corrosion pits in heat-exchanger tubes in nuclear power plants, and manufactured pits in aircraft structures, we develop general models that are suitable for analysis using **VIC-3D©** a proprietary volume-integral code. Based on these models, we develop the notion of model-based inversion, and apply it to the NDE of corrosion and pitting phenomena.

Keywords: volume-integral equations, electromagnetic nondestructive evaluation, corrosion and pitting phenomena, model-based inversion

1. Introduction

The nuclear power industry faces the serious challenge of convincing a skeptical public and regulatory agencies that it can operate safely and efficiently. Nondestructive evaluation (NDE) plays a significant role in this task, and computer modeling is playing an equally significant role in NDE. The industry now realizes the value of using such modeling to replace expensive experimental tests, as well as to design equipment, and interpret results. Eddy-currents have a traditional place in the inspection of heat exchanger tubing [1][2], and the industry seeks improved tools for such inspections.

In this paper we develop the idea of model-based inversion, that is based on the volume-integral code, **VIC-3D©**, and is briefly described in Section 2. We then develop models for real pits that have been isolated in heat-exchanger tubes in Section 3, and apply model-based inversion to these pits. The ideas are extended to pitting in aircraft structures in Section 4, and comments and conclusions are made in the final section of the paper.

2. Model-Based Inversion

2.1 VIC-3D©, A Volume-Integral Code: The foundation of model-based inversion is **VIC-3D©**[3][4], a volume-integral code for eddy-current NDE. The unknowns in the volume-integral algorithm that **VIC-3D©** uses are anomalous electric and magnetic currents, the latter occurring when either the host or anomaly (flaw), or both, are ferromagnetic with a relative magnetic permeability greater than unity. The kernels of the volume-integral functionals are vector Green functions that are computed for layered media with a variety of electromagnetic properties. The anomalies can be randomly structured, or even homogeneous, but in the latter case, we do not resort to surface-integral equations.

Embedded in **VIC-3D©**'s post-processing filter library is NLSE, the tool that drives the 'inversion-engine' for model-based inversion. The inversion process is described mathematically in (1),

$$\begin{array}{rcl} \text{Measured Data} & & \text{Model Data} \\ R_1 + jX_1 & = & f_1(p_1, p_2, p_3, \ldots, p_M) \\ R_2 + jX_2 & = & f_2(p_1, p_2, p_3, \ldots, p_M) \\ R_3 + jX_3 & = & f_1(p_1, p_2, p_3, \ldots, p_M) \\ & \vdots & \\ R_N + jX_N & = & f_N(p_1, p_2, p_3, \ldots, p_M) \ , \end{array} \tag{1}$$

where the left-hand side is a vector of measured impedances, and $p_1, \ldots, p_M$ are parameters to be determined; e.g., length, width, height of a corrosion pit. The optimization step in NLSE: Minimize $\|\mathbf{R}+j\mathbf{X}-\mathbf{f}(\mathbf{p})\|$ over $\mathbf{p}$ using Gauss-Newton iterations. The process requires **VIC-3D©** generating the model data on the right-hand side in the form of an interpolating 'look-up' table for $\mathbf{p}$.

2.2 Summary of Model-Based Inversion: The following summarizes model-based inversion:

- introduces 'Probability of Inversion'
  - how many parameters are to be inverted?
  - how large is the interpolation table for each parameter?
- does not use a variety of reference calibration blocks, with a variety of edm notches, for a variety of probe orientations
- is objective–no 'operator/inspector calls' based on *a priori* raw data
- gives an *a posteriori* estimate of sensitivity of each parameter
- gives an *a posteriori* estimate of harmful noise level
- gives a **constructive** reconstruction algorithm
- is based on a system of support algorithms, such as clutter removal, noise reduction, 'fast' models, etc.
- is robust, efficient, mathematically rigorous, and reliable.

3. Pitting Models

3.1 Pitting in a Heat-Exchanger Tube: Figure 1 show photomicrographs of actual pits in the inner-radius of Exelon PowerLabs' Braidwood Unit No. 2 heat-exchanger tube. From this, and

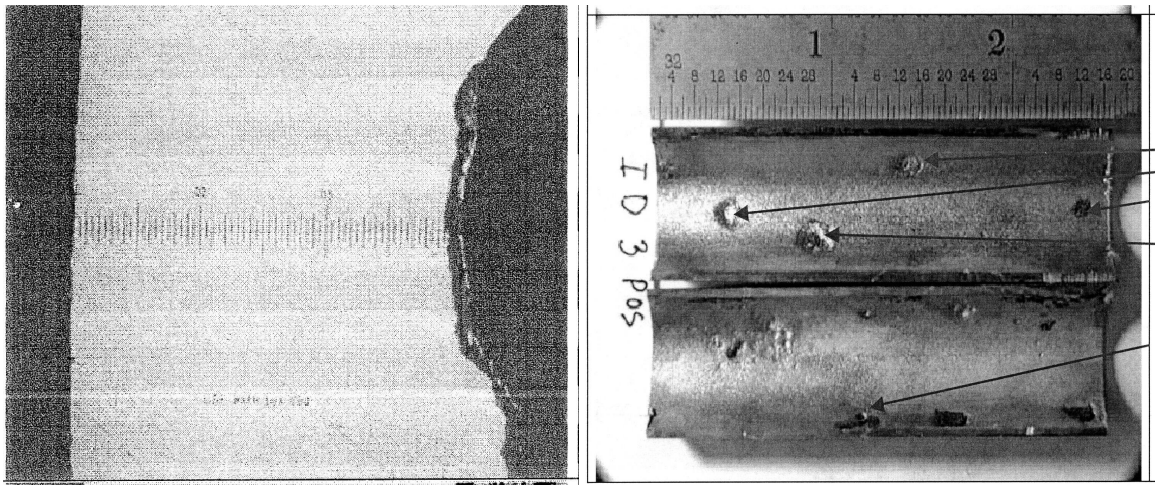

Figure 1: Photomicrographs of actual pits in Exelon's Braidwood Unit No. 2 heat exchanger tube.

similar photomicrographs, we infer that a reasonable model of such pitting are three-dimensional semi-ellipsoids that originate in the inner-radius of tube walls. Figure 2 illustrates the model, together with its three defining parameters, the semi-axes, A, B, and C.

By modeling the pit in this manner, we hope to simplify the 'inverse problem,' which is to determine the size of the pit (especially its depth) from measured data. In this case, we hope to determine the three semi-axes, thereby solving the inverse problem. Clearly, C determines the depth of the pit. From the lower photomicrograph of Figure 1, we see that the pits appear to be circular, when looking into the inner surface of the tube, with a nominal radius of 0.0625 inch. Hence, we model these pits by setting A and B equal to 0.0625. We then choose C to be equal to the difference between 0.049 inch (the nominal wall thickness) and the minimum measured wall thickness, as given in the photomicrographs.

A tube is inspected by inserting a coil co-axially to the tube (a 'bobbin coil') and then drawing it through the length of the tube. This is done over many tubes, comprising a scan of several thousand feet. The measured data are the change in impedance of the coil as it is scanned through the tube. In executing the inversion problem, we simulate measured impedance data by using model data generated by **VIC-3D©**, which were then submitted to NLSE. The output of the estimator is an estimate of the semi-axes, A, B, and C of the ellipsoidal pit, as displayed in Table 1. It only takes a few minutes to compute a table for the inversion algorithm, which is then used for all pits. Subsequently, it takes about 2-4 seconds to compute the results for each pit.

The results displayed in Table 1 indicate that the alogrithm for nonlinear estimation is reliable and robust. The maximum error occurs in A for Indication No. 8, and is only 10%, which is quite tolerable for this dimension (the width of the pit). The important point to be made from this study is the reliability in reconstructing C, the semi-axis that determines the depth of the pit. Indeed, the results of the algorithm indicate that the computation is more sensitive to depth then to the lateral dimensions, which is exactly what we're looking for!

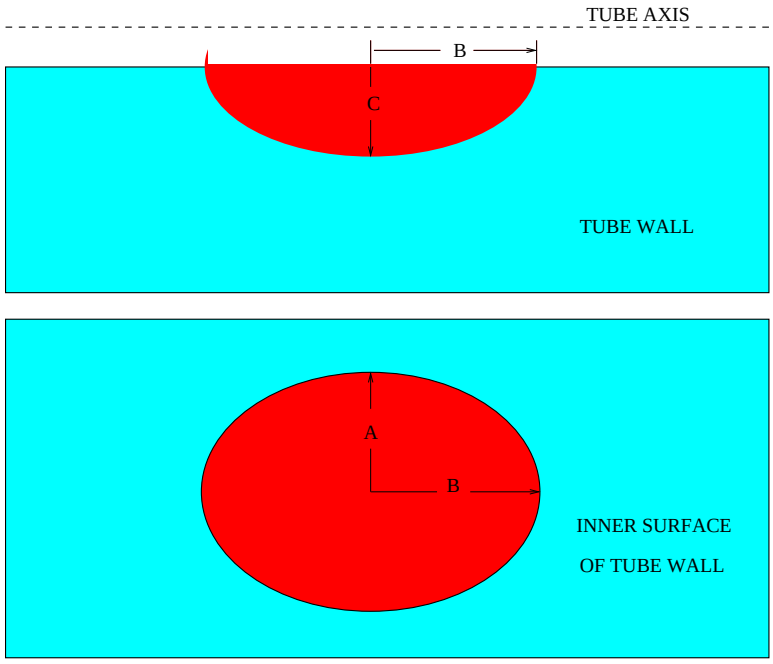

Figure 2: Illustrating a model of pits as three-dimensional semi-ellipsoids that originate in the inner-radius of a tube wall. The ellipsoid is defined by its three semi-axes, A, B, and C. A typical tube is made of copper-nickel, with $\sigma = 5.277 \times 10^6$S/m and $\mu = 1$. The outer diameter is 0.75inch, and the wall thickness is 0.049inch.

Table 1: Estimate of A, B, and C for the semi-ellipsoidal representation of the pits labeled Indication No. 3-9.

Indication	Original Model Data (in)	Reconstructed (Inverted) Data (in)
No. 3	A=0.0625, B=0.0625, C=0.026	A=0.0643, B=0.0634, C=0.0263
No. 4	A=0.0625, B=0.0625, C=0.034	A=0.0644, B=0.0639, C=0.0325
No. 5	A=0.0625, B=0.0625, C=0.029	A=0.0645, B=0.0637, C=0.0285
No. 7	A=0.0625, B=0.0625, C=0.033	A=0.0645, B=0.0639, C=0.0316
No. 8	A=0.0500, B=0.0700, C=0.034	A=0.0550, B=0.0686, C=0.0328
No. 9	A=0.0625, B=0.0625, C=0.032	A=0.0645, B=0.0639, C=0.0309

3.2 Inversion of a Complex Pit. Figure 3 illustrates a complex pit, comprising three intersecting semi-ellipsoids. The A and B semi-axes are 0.0625 inches, as before, and the C semi-axes are 0.029, 0.026 and 0.034 inches. In this exercise, we assume that the A and B semi-axes are known, as well as the locations of the centers of the semi-ellipsoids, and the job is to determine the profile-in-depth of the pit, that is, to determine the three C-axes. We use **VIC-3D©**-generated input data to NLSE at six frequencies, 10kHz, 20kHz, 40kHz, 70kHz, 200kHz, and 700kHz, with the results shown in Table 2. The interesting result is the average over the six frequencies. Clearly, the reconstruction

Table 2: Estimation of three C-axes for the complex semi-ellipsoidal pit model. The row labeled 'Freq. Avg.' is the average of the results over the six frequencies.

Freq (kHz)	Result
10	(0.026, 0.022, 0.032)
20	(0.026, 0.023, 0.032)
40	(0.026, 0.023, 0.032)
70	(0.028, 0.023, 0.033)
200	(0.032, 0.026, 0.036)
700	(0.033, 0.030, 0.037)
Freq. Avg.	(0.029, 0.025, 0.034)
True	(0.029, 0.026, 0.034)

in depth is robust, especially when frequency scanning is incorporated along with spatial scanning. The middle lobe, which is effectively lost in the presence of its two larger neighbors, is still quite accurately reconstructed.

3.3 Quantifying Corrosion Topology in Aircraft Structures–A Validation with Experimental Data: Figure 4 illustrates a corrosion topology problem that Victor Technologies was involved with for the Air Force Aging Aircraft Program. In this project actual data were taken on manufactured pits, and we developed model-based inversion algorithms to reconstruct the pits. An interpolating grid that is suitable for polynomial-spline interpolation up to order four in the two parameters, Radius and Height of the corrosion pit, is populated with 'blending functions' that are computed using **VIC-3D©**, and play the role of hardware standards in analog-based inspection. There is no use for hardware standards, analog instruments or operator intervention/interpretation in model-based inversion.

In the current inspection paradigm, in which 'Probability of Detection' ideas are used, one might be concerned about uncertainties in the host (aluminum) conductivity in Figure 4, or perhaps in the lift-off, or even tilt-angle of the probe. In model-based inversion, these 'uncertain parameters' are lumped into the unknown p's on the right-hand side of (1), and then determined along with the height and radius parameters of interest. Furthermore, NLSE will give a measure of the sensitivity of the solution to each of these variables, which is a partial-indicator of the quality of the solution.

3.4 An Algorithm for Improving Reconstructions: We have developed an algorithm that simultaneously updates the noisy measured resistance data while solving the inverse problem. The algorithm, which is illustrated in Figure 5, ultilizes the notion of projections onto convex sets (POCS).

The algorithm proceeds iteratively through a series of steps that sequentially calls NLSE to perform an inversion, **VIC-3D©** to perform a direct calculation, and an orthogonal projection to

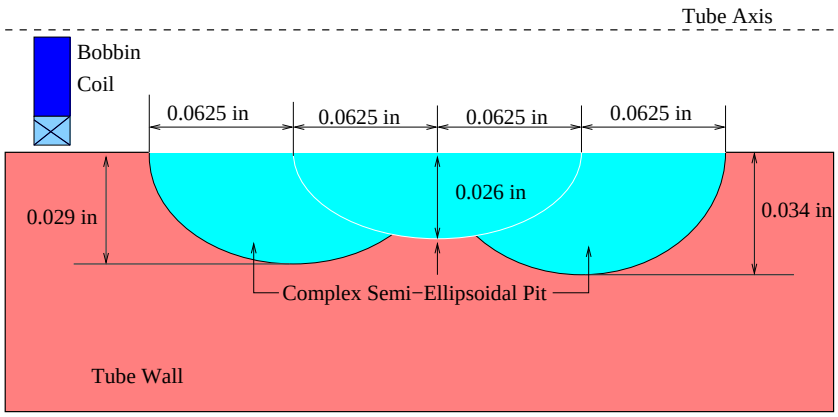

Figure 3: Illustrating a complex pit that comprises three intersecting semi-ellipsoids, whose dimensions are shown.

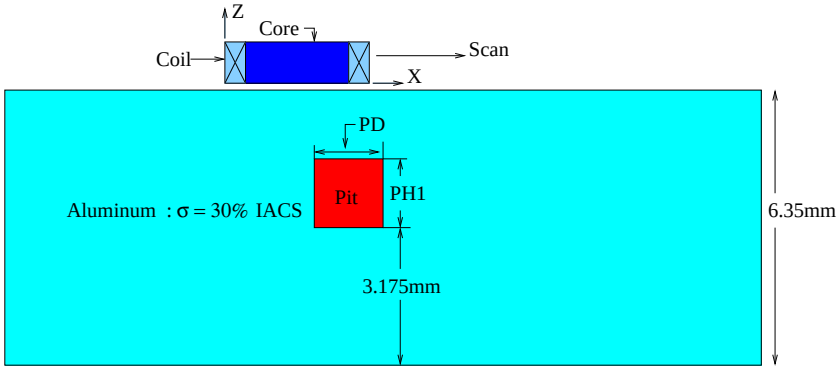

Figure 4: Quantifying corrosion topology in aircraft structures. PH1 denotes the height of a pit lying in the upper-half of the workpiece.

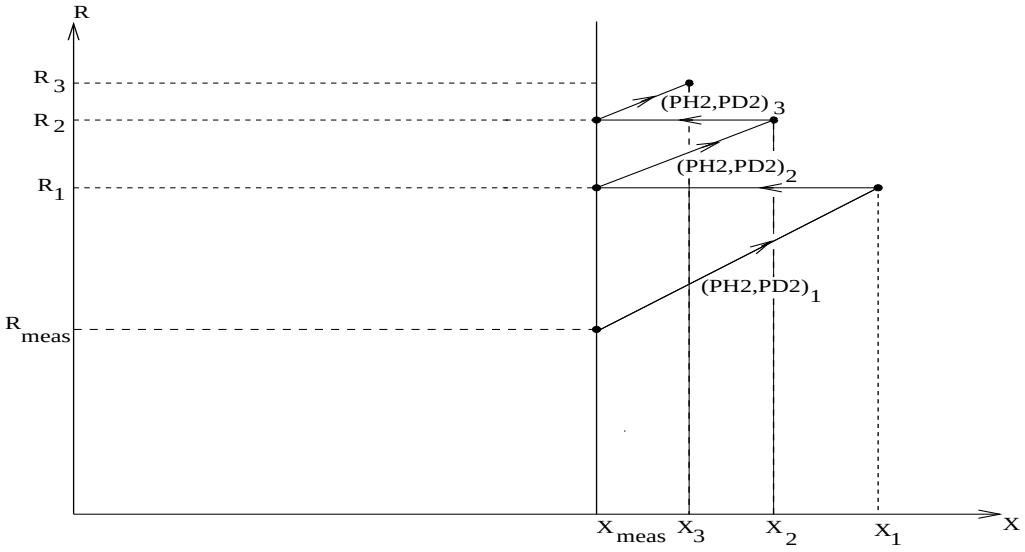

Figure 5: Illustrating the idea of projections onto convex sets (POCS) for improving resistance data during the inversion process.

return the impedance computed by **VIC-3D©** back to the straight line, $X = X_{\text{meas}}$, thus assuring that all further input data to NLSE will always have $X = X_{\text{meas}}$ as its reactance data. This ensures that the algorithm will be grounded in the more reliable component of the original measured data.

The results of running the POCS algorithm on the problem of a pit lying in the bottom-half of Figure 4 are listed in Table 3.

Table 3: Results of applying the POCS algorithm to a pit lying in the bottom-half of Figure 4. β_0 is the scale factor relating the impedance after the first iteration to the original data, β_1 is the scale factor relating the impedance after the second iteration to that after the first, and β_2 is the scale factor relating the impedance after the third iteration to that after the second. We do not go any further because β_2 is very close to unity. The 'Error' is between the final computed geometry and the 'Nominal' (experimentally determined) geometry.

NLSE STEP	(PH2,PD2)	β
0	(2.052,1.24)	$0.98757 - j0.072423$
1	(1.7884,1.3052)	$0.98852 - j0.013285$
2	(1.5528,1.3660)	$0.99960 - j0.014508$
3	(1.2625,1.4891)	
Nominal	(1.3386,1.5265)	Error: (6.0%, 2.5%)

The input impedance data generated by the POCS algorithm are shown in Figure 6. Note that the resistance data approach the 'model' with each iteration. The reactances behave in a similar manner, but do not change as strongly from iteration to iteration. Only the measured reactance data are used in each iteration. It is clear that the improvement in the reconstruction is due to the improved resistance data during the iterations. Finally, we stress that we never use the 'model' data because the model is not known to us *a priori*. Indeed, determining the model is the reason for doing the inversion in the first place.

4. Comments and Conclusions

Model-based inversion, which is playing an increasingly important role in the development of advanced techniques of electromagnetic NDE, depends crucially on the rapid solution of forward problems, and on the development of accurate models of anomalies that can be described with a few parameters. We have shown that the volume-integral approach works well within this framework, and that sophisticated inversion algorithms can be generated through the volume-integral formulation. The promise, therefore, is that model-based inversion will evolve quickly into a reliable tool for the analysis of pitting and corrosion phenomena in areas as diverse as nuclear power plants and aerospace structures.

References

[1] H. A. Sabbagh and L. D. Sabbagh, 'The Computation of Fields and Signals Due To Ferromagnetic Anomalies,' Conference Proceedings: Review of Progress in Quantitative Nondestructive Evaluation, Volume 6B, D. O. Thompson and D. E. Chimenti, eds., Plenum Press, 1987, pp. 1659-1664.

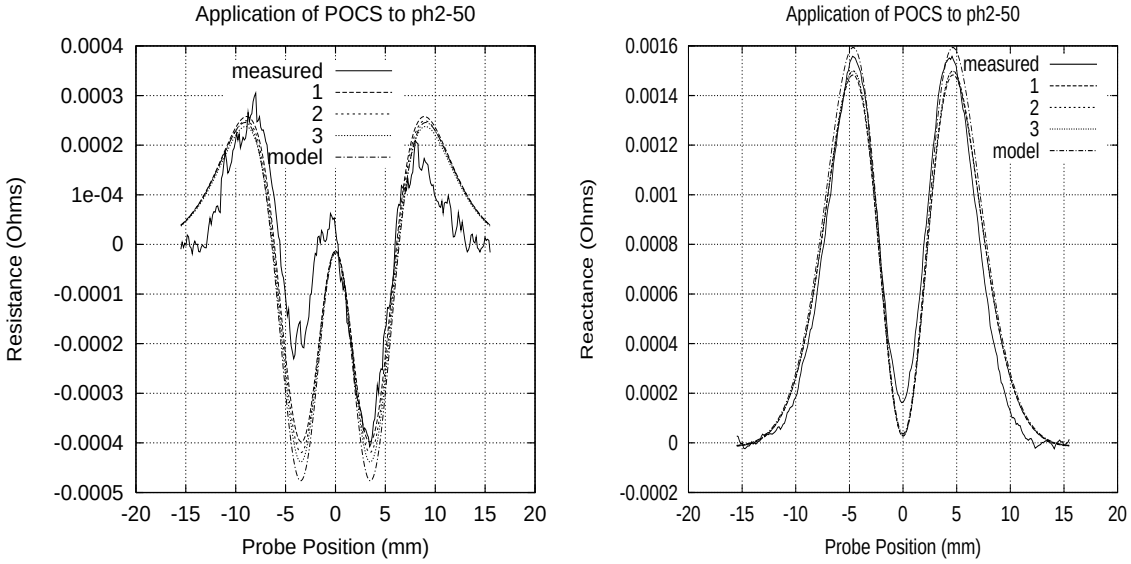

Figure 6: Input impedance data generated by the POCS algorithm applied to ph2-50, i.e., a pit lying in the bottom half of Figure 4, with a nominal height of 50% through-wall. The numbered data correspond to $(\mathrm{PH2}, \mathrm{PD2})_1$, $(\mathrm{PH2}, \mathrm{PD2})_2$ and $(\mathrm{PH2}, \mathrm{PD2})_3$ given in Table 3. Left: resistance; Right: reactance.

[2] H. A. Sabbagh, R. K. Murphy, J. C. Treece and L. W. Woo, 'Application of Volume-Integral Models to Steam Generator Tubing,' Conference Proceedings: Review of Progress in Quantitative Nondestructive Evaluation, Volume 14A, D. O. Thompson and D. E. Chimenti, eds., Plenum Press, 1995, pp. 283-289.

[3] R. K. Murphy, H. A. Sabbagh, J. C. Treece and L. W. Woo, 'A Volume-Integral Code for Electromagnetic Nondestructive Evaluation,' Conference Proceedings: 11th Annual Review of Progress in Applied Computational Electromagnetics, Monterey, CA, March 20-25, pp. 109-116, 1995.

[4] J. S. Knopp, H. A. Sabbagh, J. C. Aldrin, R. K. Murphy, E.H. Sabbagh, J. Hoffmann and G.J. Steffes, 'Efficient Solution of Electromagnetic Scattering Problems using Spatial Decomposition Algorithms,' Conference Proceedings: Review of Progress in Quantitative Nondestructive Evaluation, Volume 25A, D. O. Thompson and D. E. Chimenti, eds., American Institute of Physics, 2006, pp. 299-306.

[5] J. S. Knopp, J. C. Aldrin and P. Misra, 'Considerations in the Validation and Application of Models for Eddy Current Inspection of Cracks Around Fastener Holes,' Journal of Nondestructive Evaluation, Vol. 25, No. 3, pp. 123-138, 2006.